Metal-induced reconstruction of fullerene thin films: from dendritic to fractal growth

1998 J. Phys.: Condens. Matter 10 9609

(http://iopscience.iop.org/0953-8984/10/43/003)

J. Phys.: Condens. Matter **10** (1998) 9609–9621. Printed in the UK PII: S0953-8984(98)94064-4

Metal-induced reconstruction of fullerene thin films: from dendritic to fractal growth

J G Hou, Wentao Xu, Yongqing Li, Li Yang and Yan Wang

Structure Research Laboratory and Hefei Advanced Research Institute, University of Science and Technology of China, Hefei, Anhui 230026, People's Republic of China

Received 6 May 1998, in final form 15 September 1998

Abstract. C_{60} thin films with randomly oriented grains were grown on an (001) NaCl substrate at the substrate temperature of 160 °C. Then Ag atoms were deposited on the top of the fullerene surface in the same vacuum without changing the substrate temperature. During the deposition of the Ag, drastic changes of the film morphology and orientation were observed. By manipulating the thickness of the pristine film, different morphologies of the reconstructed C_{60} films with triangular, dendritic and fractal-like (111)-oriented single-crystal grains were obtained. A possible mechanism for this unusual reconstruction phenomenon is discussed.

1. Introduction

Since the demonstration by Krätschmer *et al* [1] that C_{60} film can be readily grown by condensation from the vapour, intense research activity has been focused on the structural and physical properties of such films [2]. The motivation for this activity is the potential for discovering new and unexpected phenomena associated with the reduced dimension of C_{60} films interacting with a wide variety of substrates. Among such interactions, those of C_{60} with metals have attracted special attention. Bulk solid solutions are formed when C_{60} interacts with the alkali and alkaline-earth metals [3–5]. For other metals deposited on C_{60} surfaces, different interactions have been reported. Cluster growth was observed for Au, In, Al and Cu deposited on C_{60} surfaces [6–10], while limited surface disruption of C_{60} and carbide formation were reported for Cr and Ti interacting with C_{60} [7, 11]. Sarkar and Halas [12] studied the diffusion of Ag in C_{60} thin films by *in situ* conductivity measurement, and suggested that Ag atoms form an impurity band in solid C_{60} with an activation energy of 0.26 eV. Wertheim and Buchanan [13] reported photoemission results for Ag–C_{60} interfacial interaction. They found that Ag donates electrons to the lowest unoccupied molecular orbital of C_{60} molecules, resulting in a metallic conduction band. However, no bulk Ag–C_{60} compound was found, since the interaction and charge transfer are confined to just one layer of C_{60} molecules in contact with the Ag. In our previous study of Ag–C_{60} composite films, ordered C_{60} nanostructures were formed between two Ag particles [14]. These results indicate that Ag–C_{60} is an interesting system; both the physical and structural properties of C_{60} are affected by the interfacial interaction between Ag and C_{60}. In this paper, we report on the observation of the film morphology and structure of C_{60} films after Ag has been deposited on their surfaces. It was found that pristine C_{60} films underwent a reconstruction process in which C_{60} aggregated into larger grains during the deposition of Ag on their surfaces if the substrate temperature was high enough. It

0953-8984/98/439609+13$19.50

is interesting that C_{60} islands have the same (111) orientation in the reconstructed films. By manipulating the thickness of the pristine C_{60} film, different film morphologies with nearly triangular, dendritic and fractal patterns were obtained. The possible driving force for this unusual re-growth process and the possible mechanism of the pattern transition are discussed.

2. Experiments and results

The samples were prepared using a two-source evaporator. The base pressure was about 1.5×10^{-5} Torr during the deposition. Before the deposition, high-purity ($\geqslant$99.9%) C_{60} was heated to 200 °C and degassed in vacuum for about half an hour. The deposition rates of the fullerene and the metal were calibrated using a quartz-crystal thickness monitor. The substrates were freshly cleaved (001) NaCl single crystals, and the temperature of the substrate was kept at 160 °C for the film deposition. Firstly, thin layers of C_{60} with different thicknesses were grown on the substrates, with a deposition rate of 0.1 nm s^{-1}, and then Ag atoms were deposited onto the C_{60} surface under the same vacuum without changing the substrate temperature. Transmission electron microscopes (TEM; Hitachi 800 and JEOL 2010) and an atomic force microscope (AFM; Park Auto Probe CP) were used for the sample characterization. Thin layers of amorphous carbon (∼5–7 nm) were deposited on top of the some C_{60}/Ag films by a sputtering method to provide a support film. Then the substrates of the films coated with carbon were dissolved in distilled water and the films were placed on copper grids for TEM observation.

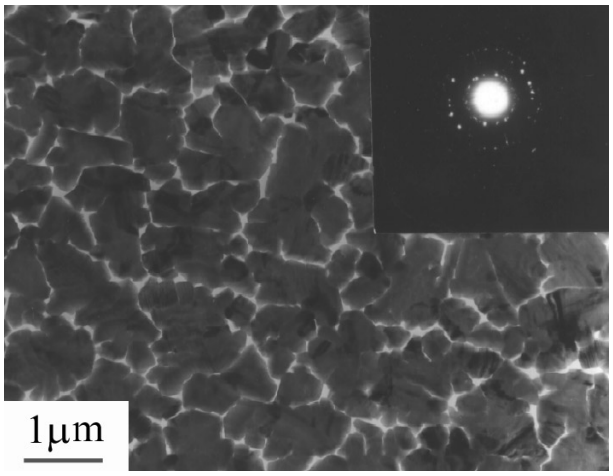

Figure 1. The TEM image and electron diffraction pattern (inset) of an as-grown polycrystalline C_{60} film 30 nm thick.

The results of the TEM observations revealed that the pristine C_{60} films grown on the (001) NaCl substrates are polycrystalline films, and this result is in agreement with the previous report [15].

Figure 1 shows the typical morphology of a pristine C_{60} film with a nominal thickness of 30 nm and the inset shows the electron diffraction pattern (EDP). From figure 1, we can find micro-crystals with sizes of about 0.5 to 0.1 μm distributed over the film, and the result from the electron diffraction indicates that these crystals are randomly oriented. The morphology and the orientation of the C_{60} film will be totally different if we deposit some

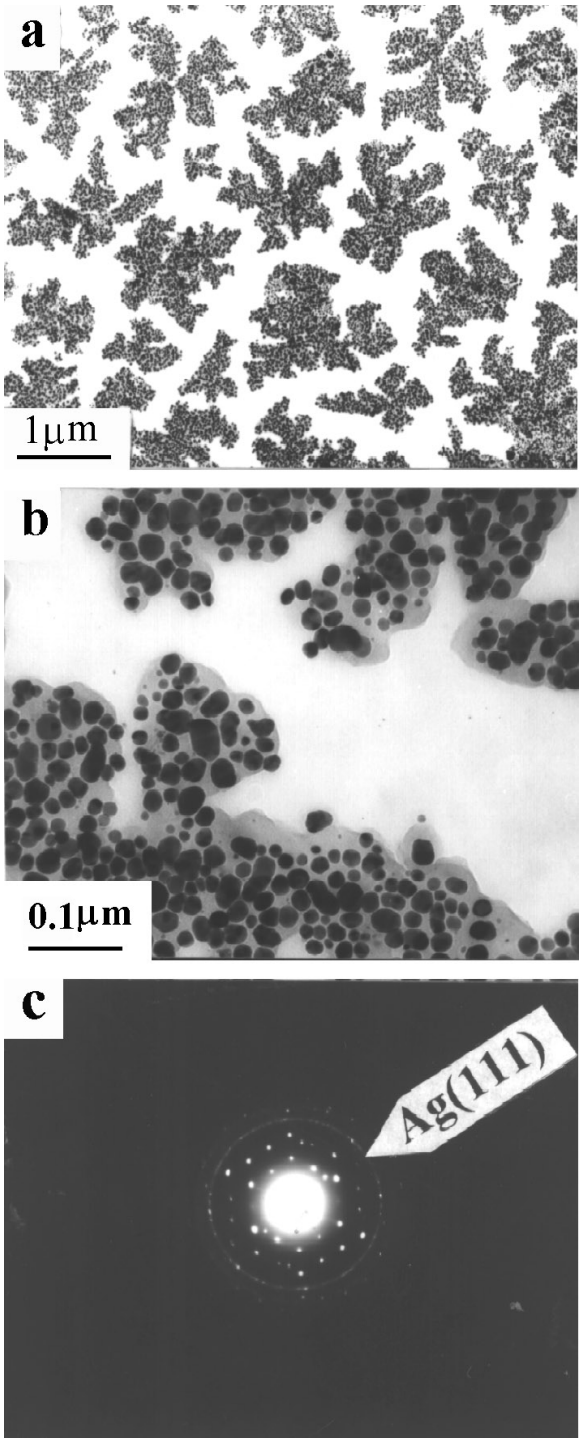

Figure 2. A low-magnification TEM image of a film 30 nm thick (sample A) after deposition of Ag (a), an enlarged TEM image of the fractal region, in which the contrast of the image is not uniform and the dark regions are Ag nano-particles (b) and the selected-area electron diffraction pattern of the fractal region (c).

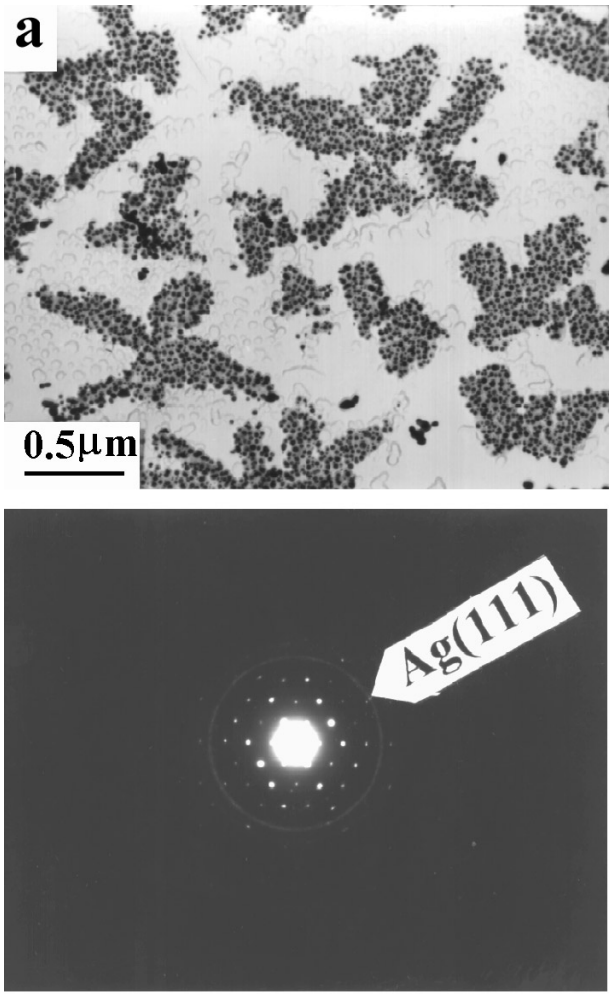

Figure 3. TEM images and electron diffraction patterns (below) for samples B, C and D with different normal thicknesses of pristine C_{60} film (see the text) after deposition of Ag. Ramified patterns were formed in sample B (a); nice dendritic patterns with threefold symmetry were obtained in film C (b); more regular patterns with nearly triangular shape were observed for sample D (c).

Ag atoms on the top of the film under the same vacuum without changing the substrate temperature.

Figure 2 shows the results for the morphology of the film of thickness 30 nm (sample A) after Ag deposition. The deposition rate of the Ag is about 0.1 nm s^{-1}, and the nominal thickness of the Ag film deposited is about 6 nm. Figure 2(a) is a low-magnification image; large fractal-like patterns with an average dimension of about 1–2 μm were formed during the deposition of the Ag. Figure 2(b) is an enlarged image of a fractal region; we can see that the image contrast of the fractal-like patterns is not uniform, and the small dark regions are Ag nano-particles. The patterns obtained by means of selected-area electron diffraction (SAED) for each fractal-like region are the same. Figure 2(c) shows a typical SAED pattern of a fractal-like region. Besides the strong (111) C_{60} spot patterns, there are

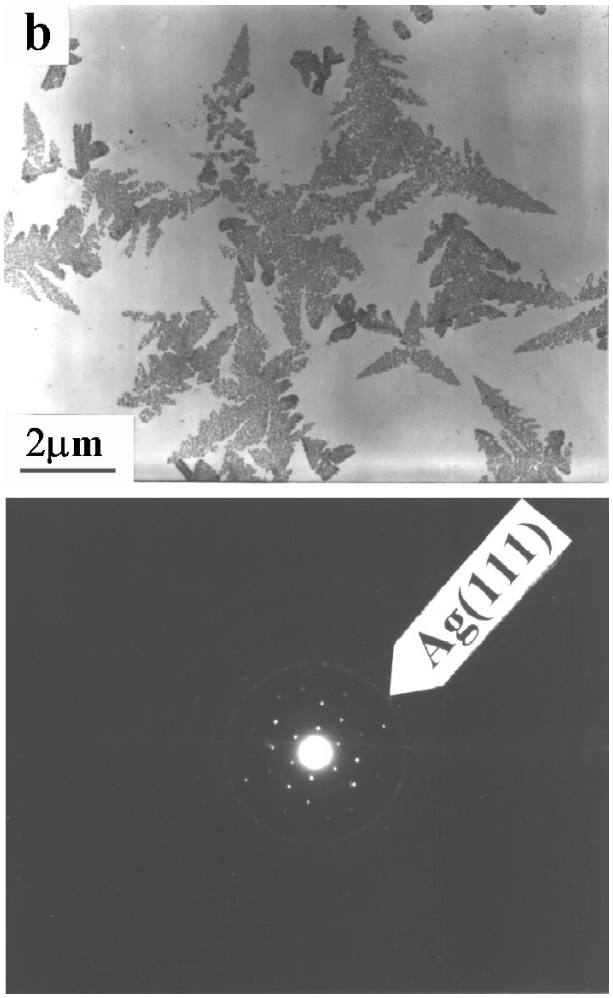

Figure 3. (Continued)

weak diffraction rings of polycrystalline Ag. We note that no C_{60} and Ag were found in the regions between the fractal patterns.

If we reduce the thickness of the pristine film, C_{60} micro-crystals with different shapes will be obtained after deposition of Ag. Several C_{60} films with nominal thicknesses of 20, 10 and 5 nm were also grown at 160 °C, and these samples will be denoted as samples B, C and D respectively in the later text. Figure 3 shows the effects of Ag adatoms on the different samples. The nominal thicknesses of Ag deposited are 3, 1 and 0.5 nm for samples B, C and D respectively. Figures 3(a), 3(b) and 3(c) are the TEM images and the SAED patterns for the corresponding samples. Random ramified patterns were still observed for sample B (figure 3(a)), although they have fewer branches compared with those of sample A (figure 2(a)). Further decrease of the thickness of the C_{60} film leads to the appearance of regular patterns after Ag deposition. Nice dendritic patterns with threefold symmetry were observed in film C (figure 3(b)), and the average dimension of the dendritic patterns is several microns, which is much larger than that of the C_{60} grains in the pristine film.

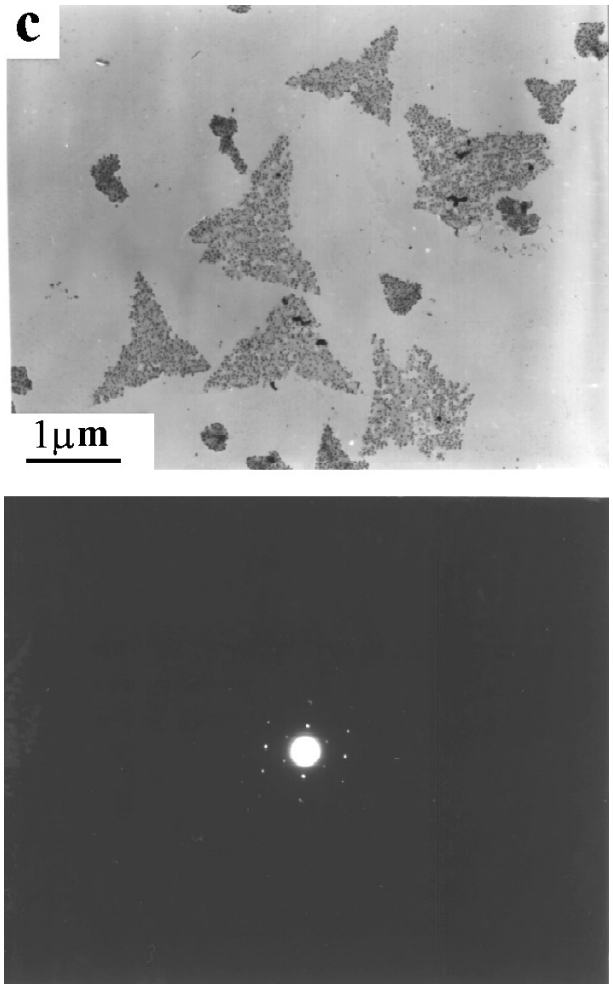

Figure 3. (Continued)

More regular patterns with nearly triangular shape (figure 3(c)) were observed for sample D. Although the shapes are quite different, the diffraction results for the C_{60}–Ag patterns in different samples are all the same: each one is a C_{60} (111)-oriented single-crystal spot pattern plus Ag polycrystalline diffraction rings. Lattice images of these C_{60}–Ag patterns were obtained by using a JEOL 2010 TEM and the results are consistent with the diffraction results.

Figure 5 shows a typical lattice image of the C_{60}–Ag patterns. The lattice fringes in figure 5 are (220) planes of C_{60} and the darker regions are believed to be Ag particles on top of or inside the C_{60} island. We note that the lattice fringes of the C_{60} cross over the Ag particles without distortion. This result suggests that Ag particles are on the surface of the C_{60} islands rather than embedded in the C_{60} matrix, and this is supported by the results of AFM studies.

Figure 6 shows an AFM image obtained from a film of 10 nm C_{60} after Ag deposition on a NaCl substrate without the carbon coating layer. Dendritic patterns were observed, like those in the TEM image (figure 3(b)). The surface of the pattern is very rough, and

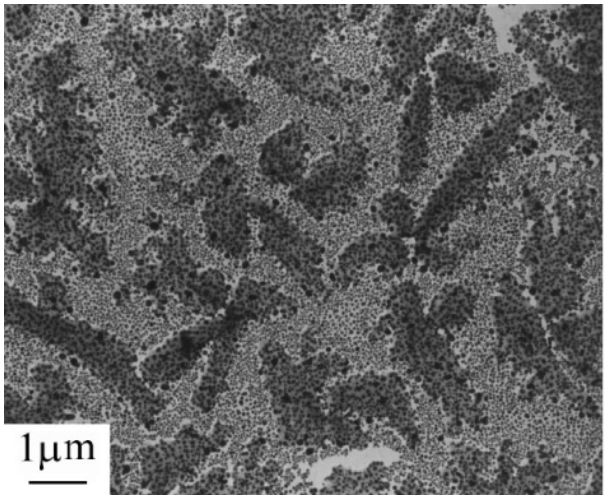

Figure 4. TEM images of a C_{60} film of 20 nm thickness after deposition of 6 nm Ag; over-deposition of Ag leads to the formation of Ag particles between the patterns.

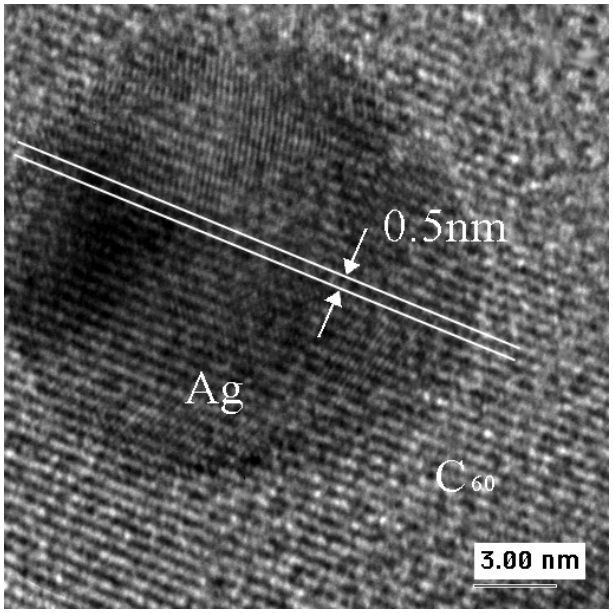

Figure 5. A high-resolution TEM image of C_{60}–Ag patterns. The round dark region is a Ag particle on top of the C_{60} film. We note that C_{60} lattices cross over the boundaries of Ag particles without distortion.

many round islands are randomly distributed within the dendritic pattern. We believe that these hilly islands are Ag particles since their dimensions are about the same as that of dark regions shown in the TEM images.

We note that the shape of the reconstructed C_{60} patterns is independent of the thickness of the Ag film, although the amounts of Ag that have to be deposited for the completion of the reconstruction are different for the C_{60} films with different thicknesses. For example, the

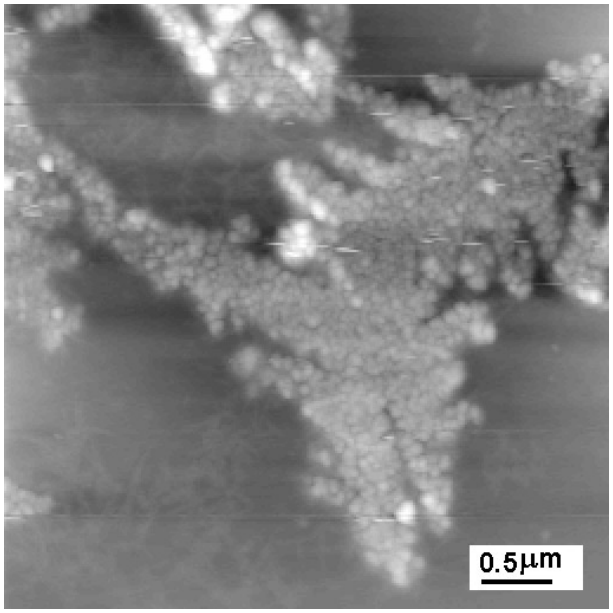

Figure 6. An AFM image of sample C after deposition of Ag.

necessary nominal thickness of Ag is about 6 nm for the C_{60} film of 30 nm thickness, while 1 nm of Ag is enough for the C_{60} film of 10 nm thickness. If we deposited more Ag than the necessary amount onto the substrate, Ag particles were formed between the fractal patterns (figure 4). We also performed experiments to study the effect of the substrate temperature on the C_{60} film reconstruction. In these experiments, the substrate temperature for the growth of a pristine C_{60} film was also kept at 160 °C, and then the substrate temperature was slowly cooled down to 100 °C for the deposition of the Ag. The results, as expected, indicate that the deposition of Ag will not cause reconstruction of the C_{60} film when the substrate temperature is low.

For a demonstration, figure 7 shows the morphology of a C_{60} film of 30 nm thickness after deposition of Ag at 100 °C. Compact patterns are observed and the orientations of these C_{60}/Ag grains are still random. As compared with the morphology of the pristine film, besides Ag nano-particles on the C_{60} surface, no significant differences were found in the size and the density of the C_{60} grains. The appearance of a few regularly shaped grains may be the result of an annealing effect imposed during the deposition of Ag.

3. Discussion

From the experimental results from TEM and AFM presented above, we can conclude that Ag adatoms lead to the reconstruction of the pristine C_{60} films when the substrate temperature is high enough. Large (111)-oriented C_{60} single-crystal islands were formed during the Ag deposition, and at the same time Ag nano-particles were formed on the C_{60} single-crystal surfaces. The average dimensions of the C_{60} crystals in the reconstructed films are much larger than those of the crystals in the pristine films, and the shapes of the patterns are only dependent on the thicknesses of the pristine C_{60} films. A transition from a random fractal pattern to a regular dendritic one was observed when the nominal thickness

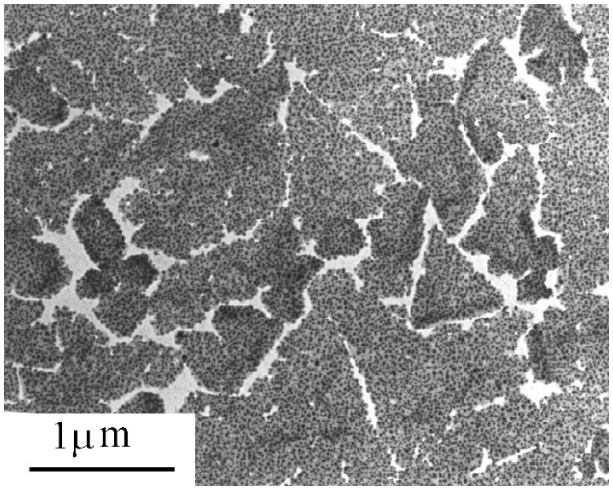

Figure 7. A TEM image of a film of 30 nm thickness after deposition of Ag at the substrate temperature of 100 °C.

of the C_{60} film decreased from 30 nm to 5 nm.

The randomly ramified (or fractal) and dendritic structures are often observed in physical, chemical and biological systems [16]. These patterns usually result from aggregation under highly non-equilibrium conditions, with material transport via diffusion-limited growth processes. The similar patterns observed in our experiment suggest that the metal-induced reconstruction of C_{60} film is also a non-equilibrium growth process. Thus, what the driving force is for the mass transport of C_{60} molecules during the deposition of Ag and why these fractal or dendritic single-crystal patterns are formed are very interesting questions. Considering the fact that pristine C_{60} film is already a stable phase, it is very important to understand the origin of the energy necessary to trigger the reconstruction of the pristine C_{60} films. The results shown in figure 2 and figure 7 indicate that substrate temperature plays an important role. However, reconstruction would not be observed if we deposited Ag on a C_{60} surface at room temperature and then annealed the sample at 160 °C for one hour.

For example, the TEM images of a C_{60} film of 20 nm thickness before and after annealing are shown in figures 8(a) and 8(b), respectively. We can see that no fractal or dendritic patterns have been formed and the orientations of the C_{60} crystals are still random, although the C_{60} grains are slightly larger after annealing. The result that larger Ag islands are formed on C_{60} surfaces indicates that significant Ag diffusion and agglomeration took place during the sample annealing. The result shown in figure 8 provides hints as regards how to achieve an understanding of the origin of the driving force of the reconstruction, since it indicates clearly that the reconstruction only happens when Ag atoms are incident onto hot C_{60} films. Furthermore, it is known that when Ag adatoms are adsorbed on the C_{60} surface, a chemical reaction takes place between Ag and C_{60} and electrons are donated to the C_{60} molecules [12]. We believe that all of the factors like the substrate temperature, the kinetic energies of the incident Ag atoms, the interaction between Ag and C_{60} and the high cohesive energy of Ag should be taken into account when discussing the mechanism of the reconstruction.

On the basis of the observed results and the above discussion, we propose a possible model to help in understanding the mechanism of the metal-induced reconstruction; figure 9

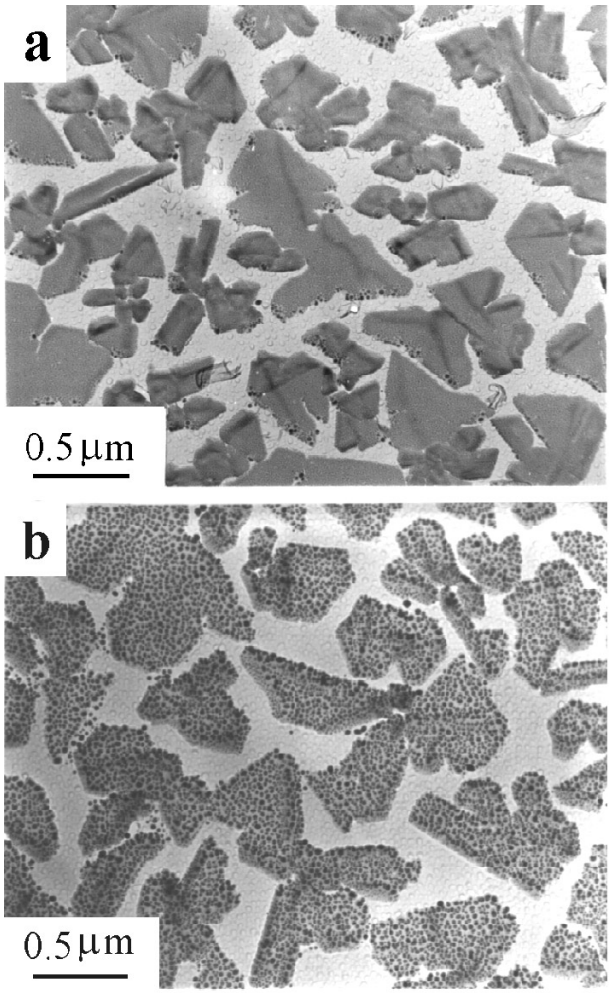

Figure 8. TEM images of a C_{60} film of 20 nm thickness after deposition of Ag at room temperature: unannealed (a); annealed at 160 °C for one hour (b).

is a schematic illustration of the model. Because of the strong interaction between Ag and C_{60} molecule, incident Ag adatoms will react with the surface layer of C_{60} molecules, and the kinetic energies will be transferred to the C_{60} lattice at the same time. On the other hand, the surface energy of the C_{60} film became very large when more and more Ag adatoms adsorbed on its surface if these Ag adatoms were not at stable nucleated sites (figure 9(a)). It is known that the binding energy of C_{60} solid is small, because of the weakness of the van der Waals force between the molecules. So it is possible that the surface energy plus the kinetic energy and the grain boundary energy of the Ag/C_{60} system is larger than the binding energy of the C_{60} lattice when the substrate temperature is high enough (160 °C). As a result, the C_{60} molecules of the pristine film become unstable and movable or, in other words, the C_{60} lattice is broken up or *melted* after interacting with the Ag adatoms at high temperature (figure 9(b)). This disordered Ag/C_{60} mixed phase is very unstable because of the very high free energy, so it has to transform to a stable phase with ordered structure. So C_{60} molecules will diffuse and be rearranged in a close-packed ordered way to form large

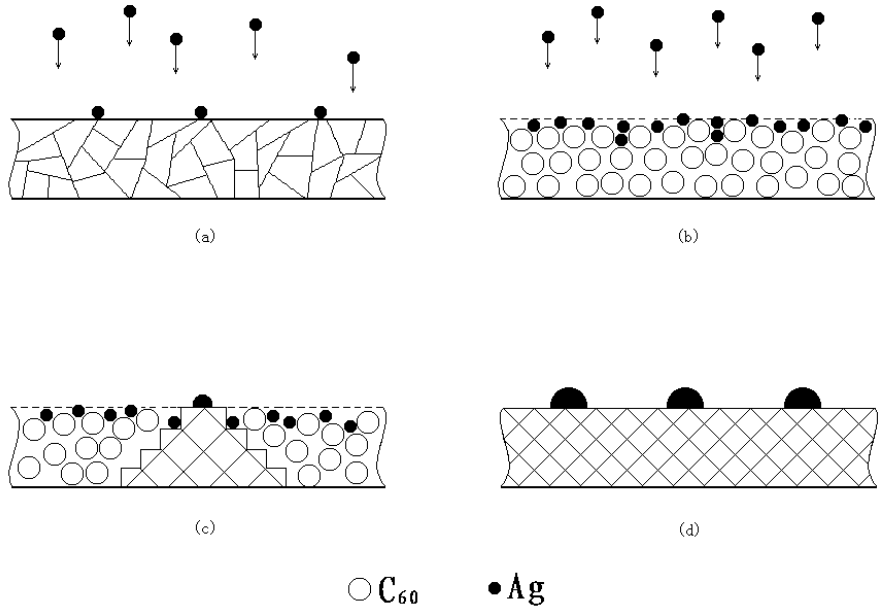

Figure 9. A schematic illustration of the process of metal-induced reconstruction of C_{60} film. Ag adatoms adsorb on the surface layer of the polycrystalline C_{60} film (a); the formation of a disordered C_{60}/Ag mixture phase as the result of the high kinetic energy and substrate temperature (b); the formation of (111)-oriented C_{60} islands and Ag clusters (c); the final stable structure is formed with Ag particles on the C_{60} (111)-oriented single-crystal surface (d).

(111)-oriented single-crystal islands, and at the same time Ag adatoms will also aggregate together to form clusters due to the high cohesive energy of Ag (figures 9(c) and 9(d)). According to the proposed model, the reconstruction only takes place when the total free energy of the Ag/C_{60} system is larger than the binding energy of the C_{60} lattice. So the results shown in figure 7 and figure 8 are understandable, because of the lower thermal vibrational energy or surface energy.

Another significant result in our experiment is the pattern transition. When the nominal thickness of the film decreases from 30 nm to 5 nm, morphological changes take place in the following sequence: random fractal $\rightarrow$ dendritic $\rightarrow$ regular crystals. So what the underlying physical factor is which is dependent on the film thickness and triggers the transition is also an interesting question. Next we will discuss briefly a possible mechanism of pattern transition.

In last few decades, extensive theoretical and experimental effort [16] has been made to discover the common underlying mechanism of pattern formation in non-equilibrium growth processes. One of the central questions is that of what causes some patterns to be dendritic and others to be fractal. In general, the transition from the fractal to the dendritic form occurs when anisotropy dominates over random noise during the growth process, and

such a transition was observed in previous studies of crystal growth by different processes such as electron chemical deposition [17], vacuum deposition [18] and crystal growth in solution [19]. In these experiments, the transition from the fractal to the dendritic form was achieved by decreasing the magnitude of the random noise. In our experiment, three kinds of stress may contribute to the anisotropy factor or the random noise that determines the shape of the growth pattern during the reconstruction. They are the surface tension related to the regular microscopic structure, the charge-transfer-induced stress and the stress of lattice misfit between the C_{60} and NaCl. The stress caused by the lattice misfit is very small, since the interaction between the C_{60} and NaCl is extremely weak [20], so the pattern transition must be determined by the other two kinds of stress. It was reported [15] that the growth rate of the (111) planes of C_{60} crystals is greater than those of the other crystal planes due to the stronger intermolecular interactions with the shorter C_{60}–C_{60} distance. The surface tension related to the regular microscopic structure is also anisotropic, and it is clear that this anisotropic surface tension favours a regular pattern which has the same threefold symmetry as the microscopic structure. Therefore triangular patterns will be formed if the surface tension is the dominant factor. On the other hand, the reconstruction is induced by Ag adatoms interacting with C_{60} in our experiment, so the charge-transfer-induced surface stress is also a very important factor. The charge-transfer-induced stress or the strain energy associated with the stress may produce a kind of local and random effect during the growth process, because Ag adatoms and small Ag clusters are randomly distributed on the C_{60} surface, and their locations as well as their sizes are time dependent during the growth process. Therefore, the formation of different patterns is the result of a competition between the anisotropic surface tension, which favours the symmetric patterns, and the charge-transfer-induced stress, which imposes a local and random force on the C_{60} growing surface. In the system of thin pristine C_{60} film, only a small amount of Ag adatoms is needed to trigger the reconstruction, so the charge-transfer-induced stress is weak, since the stress is proportional to the amount of charge transfer [21]. Under this condition, the anisotropic surface tension plays a dominant role and triangular patterns are formed. Thicker pristine C_{60} film and more Ag lead to an increase of the charge-transfer-induced stress, and finally ramified patterns are formed when this random stress becomes dominant during the growth process.

4. Conclusions

In conclusion, we have studied experimentally the effect of Ag adatoms on C_{60} thin films. If the substrate temperature was high enough, drastic morphology and orientation changes were found as a result of the deposition of Ag on C_{60} thin film. Regular, dendritic or random ramified patterns of large (111)-oriented C_{60} single-crystal grains were obtained in systems with different thicknesses of pristine C_{60} film. The pattern growth mechanism is considered as unstable interface growth, and the formation of different patterns is the result of a competition between the anisotropic surface tension and the charge-transfer-induced stress.

Acknowledgments

We thank Dr Yang Jinlong for stimulating discussion. Professor Peng Lianmao at Beijing Laboratory of Electron Microscopy, Chinese Academy of Sciences, helped us to obtain the high-resolution TEM images. This work was supported by the National Natural Science

Foundation of China (No 59529204).

References

[1] Krätschmer W, Lamb L B, Forstiropoulos K and Huffman D R 1990 *Nature* **347** 354
[2] Gruen D E (ed) 1995 *Thin Solid Films (Elsevier Science Series A)* vol 257 (Amsterdam: Elsevier) and references therein
[3] Haddon R C *et al* 1991 *Nature* **350** 320
[4] Gu C, Stepniak F, Poirier D M, Benning P J, Chen Y, Ohno T R, Martins J L, Weaver J H, Chibante L P F and Smalley R E 1992 *Phys. Rev.* B **45** 6438
[5] Kortan R, Kopylov N, Glaram S, Gyorgy E M, Ramirez A P, Fleming R M, Thiel F A and Haddon R C 1992 *Nature* **355** 529
[6] Kuk Y, Kim D K, Suh Y D, Park K H, Noh H P, Oh S J and Kim S K 1993 *Phys. Rev. Lett.* **70** 1948
[7] Ohno T R, Chen Y, Harvey S E, Kroll G H, Stepniak F, Benning P J, Weaver J H, Chibante L P F and Smalley R E 1993 *Phys. Rev.* B **47** 2389
[8] Rowe J E, Rudolf P, Tjeng L H, Malic R A, Meigs G, Chen C T, Chen J and Plummer W 1992 *Int. J. Mod. Phys.* B **6** 3909
[9] Owens D, Aldao C, Poirier D and Weaver J 1994 *Phys. Rev.* B **51** 17 740
[10] Hebard A F, Ruel R R and Eom C B 1996 *Phys. Rev.* B **54** 14 052
[11] Wang W H and Wang W K 1996 *J. Appl. Phys.* **79** 149
[12] Sarkar D and Halas N J 1993 *Appl. Phys. Lett.* **63** 2438
[13] Wertheim G K and Buchanan D N E 1994 *Phys. Rev.* B **50** 11 070
[14] Hou J G, Wang Y, Xu W, Zhang S Y and Zhang Y H 1997 *Appl. Phys. Lett.* **70** 3100
[15] Tanigaki K, Kuroshima S and Ebbesen T W 1995 *Thin Solid Films* **257** 154
[16] Vicsek T 1989 *Fractal Growth Phenomena* (Singapore: World Scientific)
[17] Grier D, Ben-Jacob E, Clarke R and Sander L M 1986 *Phys. Rev. Lett.* **56** 1264
[18] Brune H *et al* 1994 *Nature* **369** 469
[19] Honjo H, Ohta S and Matsushita M 1986 *J. Phys. Soc. Japan* **55** 2487
[20] Lurhi R, Meyer E, Haefke H, Howald L, Gutmannsbauer W and Guntherodt H-J 1994 *Science* **266** 1979
[21] Grossmann A, Erley W, Hannon J B and Ibach H 1996 *Phys. Rev. Lett.* **77** 127